Parvez A. Riza Khan
Sakhi M. Butta
Suheel A. Malik

Department of Electronic Engineering, Faculty of Engineering and Technology, International Islamic University, Islamabad, Pakistan

Modeling of Transport Properties of Amorphous Silicon Solar Cells

In this report we present the status of three projects; amorphous silicon solar cell characteristics and modeling, hole drift mobility measurements in microcrystalline and amorphous silicon, and hole-conducting polymers as p-layer materials for amorphous and crystal silicon solar cells. The work described herein was actually done on c-Si substrates, and is preliminary to work on a-Si:H based n/i structures. Fairly good c-Si/polyaniline diodes were fabricated; the open-circuit voltage under illumination was about 0.4V. The solar conversion efficiency of as-deposited pin a-Si:H solar cells can be explained surprisingly well from hole mobility and optical absorption measurements on the intrinsic layer material. We first realized this fact about 18 months ago.

***Keywords*:** Solar cells, Amorphous silicon, Interface, Transport properties
Received: 01 November 2009, **Revised**: 20 February 2010, **Accepted**: 28 February 2010

1. Introduction

We believe that we can demonstrate that the low hole drift-mobility of a-Si:H largely determines the electrical properties of as-deposited a-Si:H cells at solar illumination intensity and near room-temperature. We think it is fair to say that, despite 20 years of work on the characterization of amorphous silicon and amorphous silicon solar cells, there has been no definitive, quantitative model for how the cells work – even under restricted conditions such as the as-deposited state. Our hope for future work is that we can leverage the success of this model to gain deeper insight into the light-soaked state. The main activities in the last year have been to: (i) Obtain an improved set of J-V measurements on as-deposited a-Si:H solar cells to serve as the target for cell modeling, and (ii) to explore the range of validity of the "hole drift-mobility only" model for the as-deposited properties.

The improved set of measurements involves the use of a thickness series of cells and of a near-infrared laser to obtain uniformly absorbed illumination. Measurements were recorded over a wide range of illumination intensities. The more definitive set of measurements shows good agreement with the "hole mobility only" model for intensities ranging from 1% of AM1.5 up to AM1.5. For low intensities, this model is not very successful. It seems likely that measurements in this regime are more sensitive to deep levels such as dangling bonds.

In prior work we have obtained open-circuit voltages up to 0.73V using "PEDOT:PSS," which is a commercially available hole-conducting polymer. PEDOT:PSS uses water as its solvent; we generally deposit the polymer onto a-Si:H, and we have been concerned that oxide formation has led to reduced V_{OC}. In our present work we have been exploring doped polyaniline as the hole-conducting polymer, which uses a non-aqueous solvent.

2. Experiment

We have fabricated a simple device by spin coating a layer of conductive polyaniline onto a silicon substrate. We have considered the following relation:

$$\mu_D \equiv \frac{d^2}{2(V+V_{bi})t_T} \qquad (1)$$

where d is the i-layer thickness, V the applied voltage, V_{bi} is a correction for the internal field, and t_T is the transit-time corresponding to a charge collection of 50%

Two kinds of silicon substrates were used in this experiment: (i) n-type, orientation (100), R=2Ωcm and (ii) n-type, orientation (111), R>3000Ω.cm. We evaporated a large area, 50nm thick aluminum contact to the back (unpolished) side of the wafer. Immediately before the polymer film was applied, the silicon wafers were etched in a 2.5% HF solution.

The polyaniline base was obtained from Sigma-Aldrich Company. The solvent is dichloroacetic acid (DCA); the dopant is 2-acrylamido-2-methyl-1-propanesulphonic acid (AMPSA). The polyaniline solution was made following previous procedure [1]. The area of the spin-cast doped polyaniline film was around 0.5cm^2. The films were annealed in air at 80°C for 24 hours after casting. A circular, gold contact (50nm thick) was then evaporated onto the polyaniline film. The polyaniline films were typically 5μm thick; the resistivity of the doped

films was about $10^{-1}\Omega$.cm. The current-voltage characteristics were measured at room temperature with a Keithley 2400 source meter.

3. Results and Discussion

The work described herein is actually done on c-Si substrates, and is preliminary to work on a-Si:H based n/i structures. We were able to fabricate fairly good c-Si/polyaniline diodes; the open-circuit voltage under tungsten halogen illumination was about 0.4V. The solar conversion efficiency of as-deposited pin a-Si:H solar cells can be explained surprisingly well from hole mobility and optical absorption measurements on the intrinsic layer material. We first realized this fact about 18 months ago; at the right, we have reproduced a figure illustrating the agreement between measurements (on United Solar cells) and the model [2].

The surprise in this model is its simplicity. As has been summarized not long ago in the monograph of Schropp and Zeman [3], the standard model for undoped a-Si:H incorporates four (or more) classes of electronic states: valence bandtails, conduction bandtails, and two or more dangling bond levels. Perhaps 20 or more parameters are required if all possibly relevant electronic transport and trapping processes are treated, and veteran scientists might well despair of gaining insight from the daunting exercise of matching so many parameters to such simple measurements.

The hole drift-mobility in a-Si:H can generally be explained satisfactorily using an electronic density-of-states model with an exponential valence bandtail; these bandtail parameters are the main ones in the model. In Fig. (1), we illustrate the density-of-states; note that no defect levels are incorporated. Additionally, the conduction bandtail in this model is sufficiently narrow that it is unimportant near room-temperature; only the conduction band "effective density-of-states" N_C has a noticeable effect on the solar cell parameters, and even this effect is weak.

The relative simplicity of the proposed model is certainly refreshing, and we decided to make a more stringent comparison of cell properties with this model's predictions. As experts will no doubt recognize, graphs of power vs. thickness such as we did for Fig. (2) depend heavily upon optical properties, and one doesn't know for sure that mistakes in estimating optical effects are not being cancelled by mistakes in estimating electronic properties. For this purpose we wanted to obtain a set of cell measurements using intense, near-infrared, monochromatic laser illumination that was uniformly absorbed in the cell. Under white-light illumination, a good deal of the power generated by a single-junction cell is due to strongly absorbed illumination; models for such cells are quite sensitive to the absorption spectrum of the intrinsic and p-layers, but are less sensitive to transport and recombination properties of the intrinsic layer than are measurements with uniformly absorbed illumination.

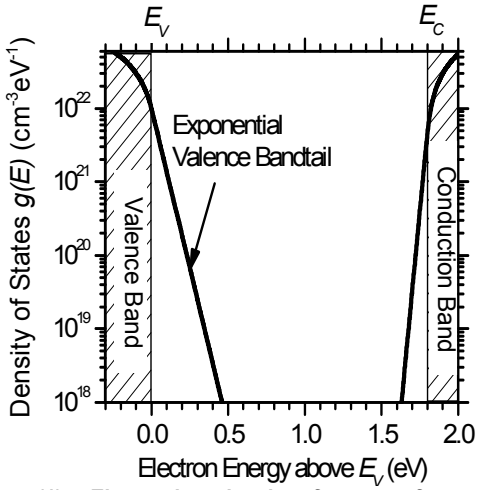

Fig. (1) Electronic density-of-states for the "bandtail" only model. The most important parameters are those of the exponential valence bandtail, since these control the (small) magnitude of the hole drift mobility

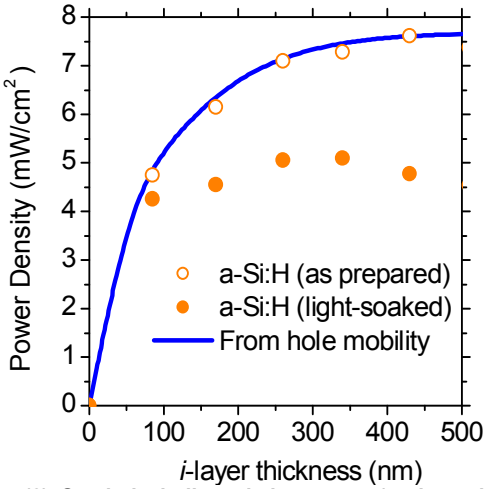

Fig. (2) Symbols indicated the power (under solar simulator illumination) for a-Si:H solar cells with varying absorber-layer thickness. The line is a model calculation encompassing hole drift-mobilities (through valence bandtail parameters), but neglecting dangling bonds and other intrinsic layer defects altogether

United Solar Ovonic LLC agreed to collaborate on these experiments, and sent us a series of samples with thickness varying from 200nm to 900nm. AM1.5 measurements were done at United Solar before the samples were sent to Syracuse. At Syracuse, we have done intensity-dependent cell measurements using illumination from a 685nm laser (absorption length about 1500nm). The model calculations used the AMPS-PC engine developed by Steve

Fonash's group at Penn State University; we used exactly the same electronic modeling parameters that we proposed previously [2]. Temperature-dependent measurements are underway as well, but will not be reported here.

In Fig. (3), we show quantum efficiency measurements as a function of i-layer thickness (i.e. the short-circuit (particle) photocurrent density J_{sc}/e normalized by the incident photon flux F). The laser wavelength λ=685nm). The solid lines are the results of "bandtail only" simulation. The simulations indicate that, for the lowest flux $F=6\times10^{13}cm^{-2}s^{-1}$, J_{sc} corresponds well to the integrated absorption of photons throughout the intrinsic-layer. The curvature noticeable for larger thicknesses is the effect of the finite absorption coefficient $\alpha=6.2\times10^{3}cm^{-1}$. As the flux is further increased (a few hundred times), there is a small additional decrease in the quantum efficiency for the thickest samples. This effect is due to recombination inside the i-layer, and is consistent with the poor fill-factors we measured (and predicted) for these thicker samples at large flux.

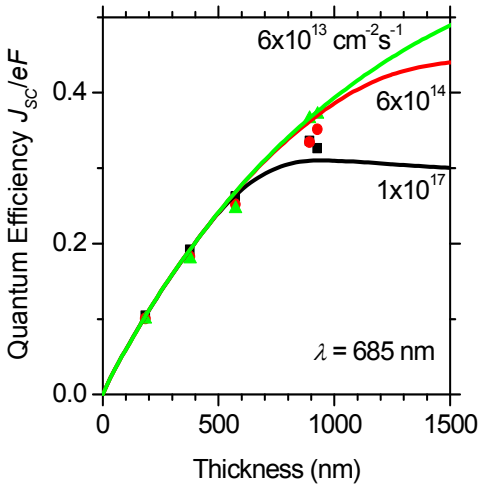

Fig. (3) The symbols indicate quantum efficiency (J_{sc}/eF) measurements for a-Si:H pin solar cells with varying thickness; results are shown for three different fluxes F. The solid lines are results from a bandtail-only calculation. (Intrinsic-layer optical parameters were $\alpha=6.2\times10^{3}cm^{-1}$, reflectivities R_f and Rb both 0.2)

In Fig. (4), we have graphed the fill-factor and open-circuit voltage measurements (symbols) and simulations (solid lines) as a function of the incident photon flux. For the fill-factors, results are shown for four different cell thicknesses. We have not shown fill-factor results for the thickest sample; although this sample was only slightly thicker than the thickest one in the illustration, it had a markedly lower fill-factor, and was plainly below the trend of the thickness series.

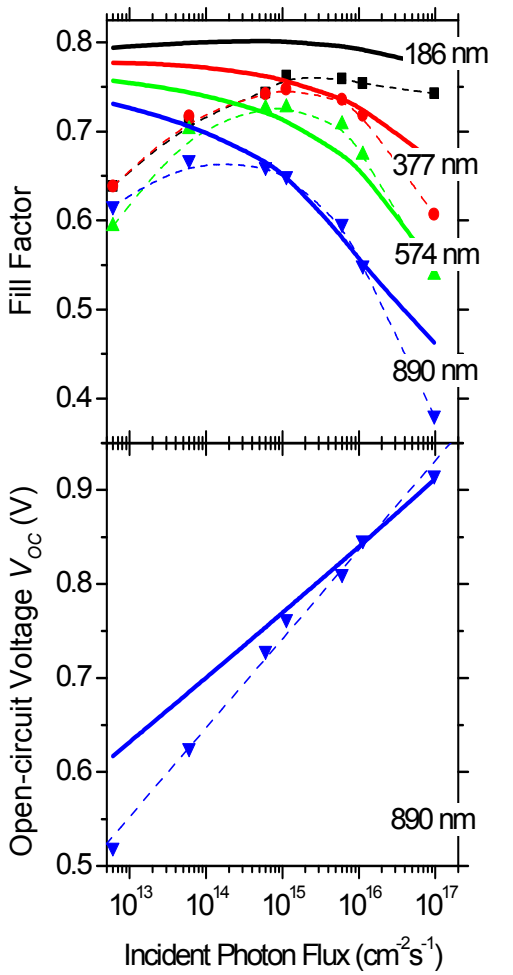

Fig. (4) Symbols indicate the intensity-dependence of the fill-factor and open-circuit voltage V_{OC} measured with uniformly absorbed illumination (685 nm) for a-Si:H pin solar cells. For the fill-factor, results for cells with four different thicknesses are illustrated. The solid lines are the cpredictions for a "valence bandtail only" model; only the optical absorption coefficient was fitted to these measurements

We have shown only a single sample to illustrate the intensity-dependence of the open-circuit voltage V_{OC}; the V_{OC} measurements have very little dependence on thickness, and for simplicity, we have shown these results separately in Fig. (5). For the higher intensities, the fill-factor declines markedly with thickness (from 0.76 to less than 0.4). The decline corresponds fairly accurately with the results of the simulations, and we are therefore fairly confident in the following qualitative explanation for the effect of thickness [3]. We start with the fact that holes have far smaller drift-mobilities than electrons; it thus takes much longer (following their photogeneration) for them to drift to the p/i interface than it takes for electrons to drift to the n/i interface. However, for thin cells, the internal electric field remains fairly large throughout the cell (even under maximum power conditions and at larger intensities). Even

ISSN 1813-2065

holes that are photogenerated close to the n/i interface are rapidly collected – both because of the larger internal field, and because of the relatively small distance between the n/i and the p/i interfaces. It is worth noting that the model predicts slightly larger fill-factors for thin cells than we measured; we don't know the reason for this (small) discrepancy.

For thicker cells, the internal electric field no longer extends across the cell, and some holes photogenerated in the "back" of the cell (i.e. closer to the n/i interface) are lost to recombination. This "collapse" of the field [4] is just a consequence of the buildup of slowly-moving, positively charged holes near the p/i interface. We gain some confidence in this view because we find that reducing the incident flux by a couple of orders of magnitude noticeably improves the fill-factor. The qualitative explanation for this effect is that, for lower incident flux, there are fewer drifting holes, and less positive space-charge to collapse the voltage. The simulations agree fairly well with the measurements for fluxes in the range 10^{15}-10^{17}.

For lower flux ($<10^{15}$cm^{-2}s^{-1}), the measured fill-factors become smaller; this is counter to the trend at high intensities, where the fill-factor decreases with increasing intensity. Furthermore, there is little difference in fill-factor for varying thickness. We do not presently have a successful model for these low-flux effects.

The bottom panel of Fig. (4) shows the intensity-dependence of the open-circuit voltage V_{OC}. The "bandtail only" model provides a good description of the measurements down to a flux of about 10^{15}cm^{-2}s^{-1}; this is essentially the same range over which the model describes the fill-factor. The corresponding photogeneration rates range from $5\text{x}10^{18}$ to $5\text{x}10^{20}$cm^{-3}s^{-1}. For lower intensities, the bandtail model deviates markedly from the measurements. Previous work by the Penn State group has shown that this low-intensity region is quite strongly affected by light-soaking [4]; we presume that a full description of the solar cell behavior will require the addition of defects to the present "bandtail only" model.

In Fig. (5), we show the thickness-dependence of the open-circuit voltage V_{OC} at several flux levels. V_{OC} is nearly independent of thickness; this essential result also emerges from the bandtail-only simulations, although there are some subtle differences in the behaviors. For thicker samples, it is relatively easy to understand thickness-independence in terms of a "quasi-Fermi level" model [2,4]. In this model, the center region of the intrinsic layer has no drift or diffusion currents; the center region is essentially a neutral photoconductor with distinct electron and hole quasi-Fermi levels E_{Fn} and E_{Fp}, respectively. The sample zones near the p/i interface essentially acts as an electrode to measure the hole quasi-Fermi level of the middle, and the n/i interface serves the same role for the electron quasi-Fermi level.

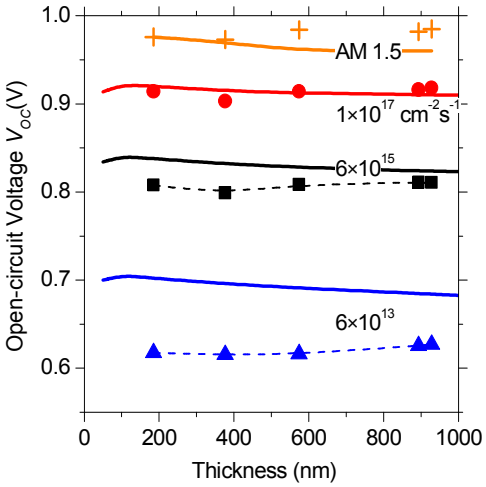

Fig. (5) The symbols represent open circuit voltages V_{OC} measured as a function of thickness for several incident flux levels (white light and 685nm). The solid lines are the results of a "bandtail" only calculation

For the moment, let us accept the validity of the basic idea proposed here: that hole drift mobilities and valence bandtails are the main elements determining the solar conversion efficiency of a-Si:H based solar cells in their a-deposited state. It is also plain that the conversion efficiency in the light-soaked state is markedly reduced from the as-deposited state, and an understanding of the light-soaked state is the ultimate goal for this research.

The role of the present work is to give a solid foundation for exploring the light-soaked state. In the third phase of this project we are making measurements on the same series of solar cells in various states of light-soaking. Surprisingly, we are unaware of any comparable series of published measurements.

We presume that we shall need to incorporate a density of dangling bonds that grows with light-soaking in order to account for the decline in conversion efficiency. We also presume that as-deposited defects will be required to accommodate the low-intensity measurements we have already made. In the spirit of the "bandtail-only" model, we shall be seeking a model with the bare minimum of additional complexity.

There have been several reports of drift-mobility measurements [4-7] in microcrystalline silicon in the last decade or so since it became clear that this material could be prepared with properties that are interesting for solar cells [4].

There is, of course, an enormous range of possible structures in microcrystalline silicon materials. For each sample there is a spectrum of sizes for the component nano and microcrystallites. Even more poorly understood, for each sample there is also a jumble of non-crystalline material that lies between the crystallites. Unsurprisingly, there has also been a very large spread in reported drift mobilities and transport properties.

In this paper we shall first summarize our recent hole drift-mobility measurements in a particular form of microcrystalline silicon that has been developed at Forschungszentrum Jülich as a solar cell absorber, and for which cells with 8.7% conversion efficiency have been reported [6]. We shall not offer a detailed defense of the measurements here, nor shall we offer an extended review and comparison with previous work on microcrystalline silicon; these will be presented elsewhere. Instead, we emphasize an unexpected aspect of the present measurements, which is that they exhibit the features of "exponential bandtail multiple-trapping."

Since its first successful application to amorphous semiconductors in the early 1980's [7], exponential-bandtail multiple-trapping (usually abbreviated as simply "multiple-trapping" or "MT") has become the standard approach to analyzing most transport experiments in hydrogenated amorphous silicon (a-Si:H) and related materials such as amorphous silicon-germanium alloys. The model assumes an exponential bandtail of localized states lying at the bottom of the conduction band, or at the top of the valence band. The application to transport also assumes the existence of a "transport edge," with the property that the only carriers that contribute to electrical transport are those occupying electronic states lying above this edge (for electrons) or below it (for holes); it has generally been assumed that this edge is the "mobility-edge" dividing localized and extended electronic states.

In the present work we have found that multiple-trapping obtains for our measurements in a predominantly crystalline form of microcrystalline silicon. This form of microcrystalline silicon is apparently a far more ordered material than amorphous silicon, and certainly X-ray measurements, Raman scattering, and direct microscopy indicate that most of the volume is associated with small crystallites. One is naturally drawn to models for electrical transport that are based on the effective-mass theory, which would seem to apply at least within a crystallite. Indeed this approach has been applied recently to Hall mobility measurements in n-type microcrystalline silicon [4]. It is thus a bit of a shock to discover that the multiple-trapping model taken from amorphous semiconductors is a better description of microcrystalline silicon than is an effective-mass based approach – but this is the implication of our measurements. The multiple-trapping parameters in the microcrystalline material do differ in interesting ways from those that have been reported for a-Si:H, and we shall return to this comparison in the concluding section of this paper.

The samples used for our measurements were pin structures prepared in designated chambers of a multi-chamber system using plasma-enhanced chemical vapor deposition at frequencies of 95MHz (VHF-PECVD) [8]. We used ZnO coated glass as a transparent, conductive substrate. The μc-Si:H(B) p-layers are about 20nm thick; the films were doped by adding trimethylboron to the silane-hydrogen gas mixture. The intrinsic μc-Si:H layers were prepared using a silane-hydrogen mixture of 5-6%. The n-layer (phosphine doped) was an amorphous a-Si:H(P) layer 30nm thick. As top contacts we used sputtered ZnO dots with diameters of 1-2mm; we plasma-etched (SF_6-gas process) the top surface of these structures to remove the n-layer from regions not under the ZnO.

In this paper we present measurements on three samples summarized in Table (1). To determine the extent of crystallinity, Raman spectra were recorded from the i-layer at spots right next to the ZnO contacts. The integrated intensity ratio $I_C^{RS} = I_C/(I_A+I_C)$ was determined by deconvoluting the spectra into three signal peaks at $480cm^{-1}$, $500cm^{-1}$ and $520cm^{-1}$. The first one can be attributed to a disordered structure like an amorphous phase or grain boundaries (I_A), and the latter two are attributed to the crystalline phase (I_C) [4].

Table (1) Sample Properties

Sample	Raman Ratio I_C^{RS}	i-layer thickness d (μm)
B	0.71	4.0
D	0.60	3.4
E	0.61	4.3

The transient photocurrents were measured in the pin diodes following illumination by a 3ns laser pulse (wavelength of 500nm) through the n-layer. The photocurrent transients were consistent with a conventional interpretation in terms of hole time-of-flight. In particular, the photocharge was independent of the applied voltage, and a transit-time was discernible in the transient. Additionally, the photocurrent at short times was linear in the applied voltage, which is consistent with transport that is linear with electric field.

 ISSN 1813-2065 Printed in IRAQ

In Fig. (6), we present our temperature-dependence measurements of the hole drift-mobility for 3 samples [5] corresponding to a particular "displacement/field" ratio ($d^2/2V$) of $7x10^{-8}cm^2/V$ of sample thickness d and applied field (V/d). The activation energy (0.13eV) is illustrative only, and does not indicate any particular depth for the bandtail traps. These average drift-mobilities, determined using $\mu_D=d^2/(Vt_\tau)$, are much larger than typically obtained in a-Si:H [6], although a direct experimental comparison at the same value for d^2/V is not possible. We compare multiple trapping fitting parameters shortly.

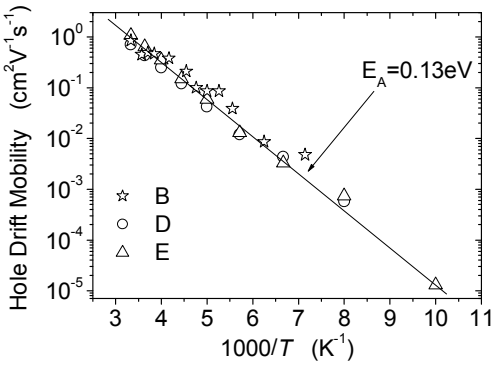

Fig. (6) Hole drift-mobilities measured for three microcrystalline silicon materials (Table 1) determined with a displacement/field ratio $d^2/2V=7.8x10^{-8}cm^2/V$

Our procedure for fitting to the multiple-trapping model starts with the transient photocharge $Q(t)$ (the time-integral of the photocurrent $i(t)$). In particular, we fit to the time-dependence of the normalized photocharge $Q(t)d^2/Q_0(V-V_{bi})$, where Q_0 is the total photocharge of holes generated by the laser pulse, V is the bias voltage, d is the i-layer thickness, and V_{bi} is a correction for the internal field. We have illustrated the photocharge measurements in Fig. (1) for seven temperatures. For clarity, we have removed sections of the transient for $Q(t)>Q_0/2$; these portions of the transient are past the "transit time," and are not used in our multiple-trapping fitting procedure. We have also removed early-time portions of the transients that are clearly dominated by response-times of the measurement.

The solid lines in Fig. (7) are the multiple-trapping fittings. The actual equation that was fitted to the normalized photocharge is [1]:

$$L(t)/E = K\left(\frac{\mu_0}{\nu}\right)(\nu t)^{\alpha(T)} \qquad (1)$$

where $L(t)$ is the mean displacement for photocarriers after a delay time t and with electric field E. The dispersion parameter $\alpha=KT/\Delta E_V$, where ΔE_V is the width of the exponential, valence bandtail, μ_0 is the valence band-mobility, and ν is an "attempt-to-escape" frequency characterizing the rate of release of holes from the bandtail traps. The constant $K=\sin(\alpha\pi)/(\alpha\pi(1-\alpha))$ is of order unity. The multiple-trapping parameters we chose (and that are the basis for the solid lines shown in Fig. 1) are given in Table (2) below, along with some results for a-Si:H [1,7].

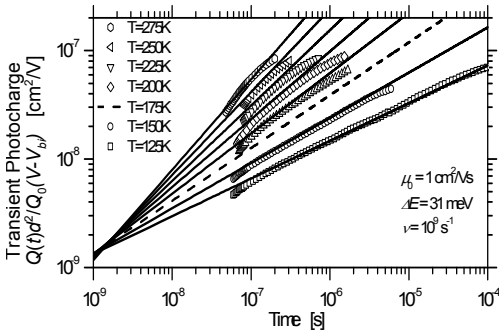

Fig. (7) The symbols are normalized photocharge transients measured in one microcrystalline silicon sample ("D" in Table 1); the solid lines are the corresponding calculations using the exponential bandtail multiple-trapping model with the parameters indicated

Table (2) Multiple-trapping fitting parameters

Multiple-trapping parameter	μc-Si:H (this work)	a-Si:H [17]	a-Si:H [18]
Valence band-mobility μ_0 (cm^2/Vs)	1.0	0.7	0.3
Bandtail width ΔE_V (meV)	31	45	48
Attempt-frequency ν (s^{-1})	$9x10^8$	$1x10^{12}$	$8x10^{10}$

One approach to analyzing mobilities in polycrystalline materials is to invoke the effective masses that would obtain for electrons and holes in the single crystal, and assume that the grain boundaries act as scatterers or barriers and as the locus for traps for the carriers [9]. It is instructive to use this approach crudely to calculate an "effective-mass carrier mobility" for holes $\mu_h^{e.m.}$ utilizing the expression $\mu_h^{e.m.}=v_{th}l/(kT/e)$, where v_{th} is the "thermal velocity" for holes (about 10^7cm/s in c-Si near room-temperature) [1] and l is a scattering length. If the scattering length is identified with a typical crystallite size of 3nm, we infer $\mu_h^{e.m.}=120cm^2/Vs$, or about 100 times larger than the estimate in Table (1). The effects of traps and barriers seem unlikely to explain the discrepancy for our samples, since these were already (implicitly) incorporated in the analysis that led to the estimate $\mu_0=1cm^2/Vs$.

We suggest that, for our samples of microcrystalline silicon, the disorder is sufficient to strongly alter the bandedge states from their

crystalline counterparts. In particular, we suggest that the bandedge states of the crystal have been transformed into a bandtail (i.e. that the density-of-states $g(E)$ has been altered), and that a mobility-edge has formed within the bandtail [10] (i.e. states lying deeper in the energy gap are localized).

The mobility-edge has been widely applied to amorphous semiconductors [11,12], and has recently been applied to microcrystalline samples with a larger fraction of amorphous "tissue" [13]. Here we are suggesting that it be applied to samples that are predominantly crystalline. In the mobility-edge model, hole states with energy levels below the mobility-edge ($E<E_V$) are completely delocalized (by definition), although with very different wavefunctions than the effective-mass states of crystals. Hole states lying above the mobility-edge ($E>E_V$) are localized. Both analytical and computational studies of mobility-edges [14,15] indicate that the localization radius for a hole state grows very rapidly, and may even diverge, as the state's energy approaches the mobility-edge. It isn't clear theoretically how particular atomic-scale features such as "strained bonds" are incorporated into the bandtail states.

With this perspective, we first discuss the bandtail width ΔE_V. The estimate of 31meV for the microcrystalline material seems unremarkable in the context of work on holes in amorphous silicon, which yield values in the range 40-50meV. It is worth noting that disorder affects holes and electrons very differently. The conduction bandtail in amorphous silicon has a width around 22meV [12,16]. Electron properties in samples quite similar to the present ones have been studied using post-transit time-of-flight [17]; bandtail multiple-trapping did not apply for these transients. An interesting possibility is therefore that electron transport may be governed by effective masses in exactly the same material for which holes require a mobility-edge approach.

The fact that the hole band-mobility μ_0 is about the same in the present microcrystalline samples and in amorphous silicon seems to support the mobility-edge interpretation, and more broadly suggests that a value near 1 cm^2/Vs may be a universal property of a mobility edge. Such "universality" is also suggested by the fact that electron band-mobilities in amorphous silicon are also around $1cm^2/Vs$ [12,16]. Interestingly, a band mobility of $1cm^2/Vs$ is not an obvious implication of the existing theoretical treatments of mobility-edges.

Finally, we turn to the attempt-frequency ν. It is quite interesting that the value for microcrystalline silicon is substantially (about 100 times) smaller than the lower values reported for a-Si:H. However, even for a-Si:H, there is no well-accepted physical interpretation for this parameter. One often-mentioned interpretation is that ν be identified as a "typical phonon frequency," but this association fails to explain either the very low magnitudes or the enormous range of magnitudes that have been reported experimentally [12]. Yelon and Movaghar have suggested that multi-phonon effects lead to the variations, and this perspective has been applied by Chen *et al.*, to drift-mobility measurements [18]. Another possibility originating with high-field drift-mobility measurements in a-Si:H has been that ν reflects the bandedge density-of-states $g(E_V)$ [19], which suggests that the present measurements be interpreted as indicating a substantially lower value for $g(E_V)$ in microcrystalline than in amorphous silicon. Plainly, we need more clues from experiment about the meaning of this parameter; it seems possible that its dramatic lowering in microcrystalline silicon could be providing it.

4. Conclusion

In this article, we present the status of three projects; amorphous silicon solar cell characteristics and modeling, hole drift mobility measurements in microcrystalline and amorphous silicon, and hole-conducting polymers as p-layer materials for amorphous and crystal silicon solar cells. In the present work we have found that multiple-trapping obtains for our measurements in a predominantly crystalline form of microcrystalline silicon.

References

[1] S. Dinca, G. Ganguly, Z. Lu, E.A. Schiff, V. Vlahos, C.R. Wronski and Q. Yuan, in Amorphous and Nanocrystalline Silicon Based Films, edited by J.R. Abelson, G. Ganguly, H. Matsumura, J. Robertson, E.A. Schiff (Materials Research Society Symposium Proceedings Vol. 762, Pittsburgh, 2003), 343.

[2] K. Zhu, J. Yang, W. Wang, E. A. Schiff, J. Liang and S. Guha, in Amorphous and Nanocrystalline Silicon-Based Films, edited by J.R. Abelson, G. Ganguly, H. Matsumura, J. Roberstson, and E.A. Schiff (Materials Research Society Proceedings Vol. 762, Pittsburgh, 2003), 297.

[3] R.E.I. Schropp and M. Zeman, "Amorphous and Microcrystalline Silicon Solar Cells: Modeling, Materials, and Device Technology", Kluwer Publishing Ltd. (Boston) (1998).

[4] E.A. Schiff, *Solar Ener. Mater. Solar Cells*, 78 (2003) 567-595.

 ISSN 1813-2065 Printed in IRAQ

[5] Q. Wang, R.S. Crandall and E.A. Schiff, in Conference Record of the 21st Photovoltaics Specialists Conference (IEEE, 1996), 1113.
[6] J. Pearce, R. Koval, A. Ferlauto, R. Collins, C. Wronski, J. Yang and S. Guha, *Appl. Phys. Lett.*, 77 (2000) 19.
[7] T. Tiedje, *Appl. Phys. Lett.*, 40 (1982) 627.
[8] O. Vetterl, A. Dasgupta, A. Lambertz, H. Stiebig, F. Finger and H. Wagner, Mater. Res. Soc. Symp. Proc., 664 (2001) A25.8.
[9] T. Weis, R. Lipperheide, U. Wille and S. Brehme, *J. Appl. Phys.*, 92 (2002) 1411.
[10] G. Juška, M. Viliūnas, K. Arlauskas, N. Nekrašas, N. Wyrsch and L. Feitknecht, *J. Appl. Phys.*, 89 (2001) 4971.
[11] M. Serin, N. Harder and R. Carius, J. Mater. Sci.: Materials in Electronics 14 (2003) 733.
[12] T. Tiedje, in Hydrogenated Amorphous Silicon II, edited by J.D. Joannopoulos and G. Lucovsky (Springer-Verlag, New York, 1984), pp. 261-300.
[13] T. Dylla, F. Finger, E. A. Schiff, *unpublished results*.
[14] J. Meier, R. Flückiger, H. Keppner and A. Shah, *Appl. Phys. Lett.*, 65 (1994) 860.
[15] O. Vetterl, A. Dasgupta, A. Lambertz, H. Stiebig, F. Finger and H. Wagner, Mater. Res. Soc. Symp. Proc., 664 (2001) A25.8.
[16] Q. Wang, H. Antoniadis, E.A. Schiff and S. Guha, *Phys. Rev. B*, 47 (1993) 9435.
[17] S. Reynolds, V. Smirnov, C. Main, R. Carius and F. Finger, in Amorphous and Nanocrystalline Silicon Based Films, edited by J.R. Abelson, G. Ganguly, H. Matsumura, J. Robertson, E.A. Schiff (Materials Research Society Symposium Proceedings Vol. 762, Pittsburgh, 2003), 327.
[18] T. Weis, R. Lipperheide, U. Wille and S. Brehme, *J. Appl. Phys.*, 92 (2002) 1411.
[19] L. Houben, M. Luysberg, P. Hapke, R. Carius, F. Finger and H. Wagner, *Phil. Mag. A*, 77 (1998) 1447.

